Journal of Breast Cancer

J Breast Cancer 2013 March; 16(1): 90-96 http://dx.doi.org/10.4048/jbc.2013.16.1.90

ORIGINAL ARTICLE

Dose Reduction in Automatic Optimization Parameter of Full Field Digital Mammography: Breast Phantom Study

Myung-Su Ko, Hak Hee Kim[1], Joo Hee Cha[1], Hee Jung Shin[1], Jeoung Hyun Kim[2], Min Jeong Kim

Health Screening and Promotion Center, Asan Medical Center, Seoul; [1]Department of Radiology and Research Institute of Radiology, Asan Medical Center, University of Ulsan College of Medicine, Seoul; [2]Department of Radiology, Kyung Hee University Hospital at Gangdong, Kyung Hee University College of Medicine, Seoul, Korea

Purpose: We evaluated the impact of three automatic optimization of parameters (AOP) modes of digital mammography on the dose and image quality. **Methods:** Computerized Imaging Reference Systems phantoms were used. A total of 12 phantoms with different thickness and glandularity were imaged. We analyzed the average glandular dose (AGD) and entrance surface exposure (ESE) of 12 phantoms imaged by digital mammography in three modes of AOP; namely standard mode (STD), contrast mode (CNT), and dose mode (DOSE). Moreover, exposure factors including kVp, mAs, and target/filter combination were evaluated. To evaluate the quality of the obtained digital image, two radiologists independently counted the objects of the phantoms. **Results:** According to the AOP modes, the score of masses and specks was sorted as CNT > STD = DOSE. There was no difference in the score of fiber among the three modes. The score of image preference was sorted as CNT > STD > DOSE. The AGD, ESE, and mAs were sorted as CNT > STD > DOSE. The kVp was sorted as CNT = STD > DOSE. The score of all test objects in the phantom image was on a downtrend with increasing breast thickness. The score of masses was different among the three groups; 20-21% > 30% > 50% glandularity. The score of specks was sorted as 20-21% = 30% > 50% glandularity. The score of fibers was sorted as 30% > 20-21% = 50% glandularity. The score of image preference was not different among the three glandularity groups. The AGD, ESE, kVp, and mAs were correlated with breast thickness, but not correlated with glandularity. **Conclusion:** The DOSE mode offers significant improvement (19.1-50%) in dose over the other two modes over a range of breast thickness and breast glandularity with acceptable image quality. Owning knowledge of the three AOP modes may reduce unnecessary radiation exposure by utilizing the proper mode according to its purpose.

Key Words: *Breast, Imaging phantom, Mammography, Radiation dosage*

INTRODUCTION

Breast cancer is the most commonly diagnosed cancer in women and is the most common cause of cancer death in women [1]. Mammography is considered as the most effective method for detecting early-stage breast cancer [2]. For this reason, mammographic examinations are performed for screening as well diagnosis. However, with the increase in screening mammographic examinations, the carcinogenic risk associated with the ionizing radiation of mammography and the absorbed radiation applied to the breast is a concern. For this reason, assessing the dose of energy to the breast during mammography is important.

After the approval of the digital mammography system by the U.S. Food and Drug Administration (FDA) in January 2000, digital mammography systems have been rapidly replacing screen-film mammography systems. The increase in the use of digital mammography systems has necessitated a revisit to the issue of screening mammography technique optimization, given the removal of limitations of mammographic film in latitude and display contrast, detection efficiency, storage, dissemination, and operating efficiency [3,4].

Most digital mammography systems have an automatic beam quality selection mode (automatic optimization of parameters, AOP) with an automatic exposure control (AEC), which automatically selects kVp, milliampere-seconds (mAs), target material, and filter, in order to control for the appropriate amount of radiation for an acceptable low dose and an increased

Correspondence to: Hak Hee Kim
Department of Radiology and Research Institute of Radiology, Asan Medical Center, 88 Olympic-ro 43-gil, Songpa-gu, Seoul 138-736, Korea
Tel: +82-2-3010-4352, Fax: +82-2-476-0090
E-mail: hhkim@amc.seoul.kr

Received: August 28, 2012 **Accepted:** January 31, 2013

http://ejbc.kr | pISSN 1738-6756 eISSN 2092-9900

contrast, according to breast thickness and composition, in terms of glandularity, i.e., the average fraction of glandular tissue, as well as the preadjustment of settings for the lowest possible dose or highest possible image contrast, according to user preference.

Improvement in signal-to-noise ratio (SNR) and the development of digital systems allow for a dose reduction in digital mammography [5,6]. However, the recommended radiation dose used for digital mammography is generally equivalent to that of screen-film mammography, which is less than 3 mGy per view, as stated by the American College of Radiology (ACR). The reason that the recommended dose has not been modified for newer systems may be because the relationship between image quality and dose has not been well established in digital mammography systems.

Although previous studies [7-9] have used the AOP mode to assess the relationship between mammographic beam quality and dose reduction, the relationship between image quality and dose differences among the three AOP modes are not well-defined. The purpose of our study was therefore to evaluate the impact of the three AOP modes on image quality and dose over a range of breast thickness and breast glandularity.

METHODS

Mammography systems

This study was performed using three digital mammography machines; two Senographe 2000DS and a Senographe Essential, both manufactured by General Electric Healthcare (Milwaukee, USA). Senographe systems have a dual track X-ray tube with a molybdenum (Mo) and a rhodium (Rh) anode track and a 0.03 mm Mo and a 0.025 mm Rh filter. They are indirect type flat-panel detectors (CsI), which have the same del size (100 μm) but a different detector size: Senographe Essential, 24×30.7 cm^2 and Senographe DS, 23×19.2 cm^2. The Senographe digital mammography system can operate in three different modes of AOP: contrast (CNT), standard (STD), and dose (DOSE) modes, which vary in the balance between low dose and high image quality. The CNT mode emphasizes higher contrast and therefore, higher image quality. The DOSE mode focuses on dose reduction with acceptable image quality. The STD mode emphasizes a compromise between good contrast and dose reduction. In each mode, the system allows a 15 millisecond pre-exposure in order to evaluate the absorption measurement so as to select the optimal parameters (target, filter, kVp, and mAs) for the final exposure. During the pre-exposure, the system also selects a 1×1 cm subregion of the 14×15 cm AOP detector area that serves as the active AEC sensor during the exposure that follows. The system selects the specific 1×1 cm subregion that records the lowest signal during pre-exposure. The full exposure is terminated when the selected 1×1 cm region records an adequate signal, thereby helping to ensure an adequate signal and a SNR to the entire image according to the technique choice preference [10].

We used a GE system (General Electric Healthcare) with two 5-million-pixel gray-scale liquid crystal display monitors. The maximum luminance of the monitors was 700 cd/m^2. The resolution was 2,048×2,560 pixels and the pixel pitch was 0.165 mm. The window width and level settings of the digital images were adjusted to optimize the image display.

Breast phantom

The Computerized Imaging Reference Systems (CIRS) tissue-equivalent mammography QA phantoms (Model 012A; CIRS Inc., Norfolk, USA) of breast equivalent material at different thickness and composition were used (Figure 1). Phantoms are breast-shaped and made of epoxy resin with a standard thicknesses of 4, 5, and 6 cm, equivalent to 50%, 30%, and 20% glandular breast tissue, respectively, in terms of its X-ray attenuation properties. In addition, compensation plates can increase by 0.5 cm, equivalent to 30%, 50%, and 70% glandular breast tissue, respectively, to the simulated breast lesions of different thicknesses.

By using a combination of different tissue composition phantoms and compensation plates, the overall glandularity was calculated using the following formula:

$$\% \text{ glandularity} = (\Sigma D_i T_i)/\Sigma T_i \text{ [11]}$$

where D_i is the percent glandularity of the i^{st} phantom (or compensation plate), and T_i is the thickness of the i^{st} phantom (or compensation plate).

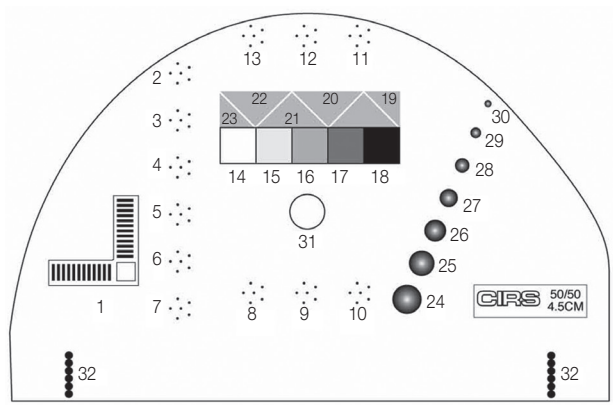

Figure 1. Schematic diagram of a Computerized Imaging Reference Systems (CIRS) phantom. The phantom breast detail component consists of 12 $CaCO_3$ specks groups of different sizes, 7 hemispheric masses of different diameters, and 5 nylon fibers of different diameters.

The phantom breast detail component consists of 12 $CaCO_3$ specks groups of varying sizes, seven hemispheric masses of varying diameters, and five nylon fibers of varying diameters. The diameters of the $CaCO_3$ specks from No.2 through No.7 in a vertical line are 0.130, 0.165, 0.196, 0.230, 0.275, and 0.400 mm, respectively. The diameters of $CaCO_3$ specks from No.8 through No.10 in the posterior transverse line are 0.230, 0.196, and 0.165 mm, respectively. The diameters of the $CaCO_3$ specks from No.11 through No.13 in the anterior transverse line are 0.230, 0.196, and 0.165 mm, respectively. The diameters of the hemispheric masses from No.24 through No.30 are 4.76, 3.16, 2.38, 1.98, 1.59, 1.19, and 0.90 mm, respectively. The diameters of the nylon fibers from No.19 through No.23 are 1.25, 0.83, 0.71, 0.53, and 0.30 mm, respectively.

Data acquisition

We used 12 phantoms types: six phantoms of 50% glandular breast tissue with 4.0, 4.5, 5.0, 5.5, 6.0, and 6.5 cm breast thicknesses, four phantoms of 30% glandular breast tissue with 5.0, 5.5, 6.0, and 6.5 cm breast thickness, one phantom of 20% glandular breast tissue with 6.0 cm breast thickness, and one phantom of 21% glandular breast tissue with 6.5 cm breast thickness. The last phantom was composed of 20% glandular breast tissue with 6.0 cm breast thickness and a compensation plate of 30% glandular breast tissue with 0.5 cm breast thickness. These 12 phantoms were imaged using the three Senographe digital mammography systems; three images were obtained per phantom type using three different AOP modes: CNT, STD, and DOSE mode. A total of 108 images were obtained. The Senographe systems include the parameters for each exposure in the image Digital Imaging and Communications in Medicine (DICOM) header. The information relevant to this study, included in the DICOM header, was stored in the fields related to X-ray generation and acquisition (kVp, exposure [unit: mAs]), anode target material, filter material, exposure control mode, average glandular dose (AGD), and entrance surface exposure (ESE). AGD is the average absorbed dose in the glandular tissue (excluding skin) in a uniformly compressed breast [12]. The entrance surface exposure and AGD for each mammography were automatically calculated from the tube output (kVp and target/filter combination) and the tube loading (mAs) stored in the DICOM header of each image. We extracted the necessary data from the header and stored them in a database.

All readings were performed in a dark environment suitable for interpreting the mammograms.

CIRS phantom images were examined and scored according to the three features: $CaCO_3$ specks, hemispheric masses, and nylon fibers. The scoring criteria for each detail of the CIRS phantom images were based on the guidelines by the American College of Radiology (ACR), which is a three-step point visibility scale (0, 0.5, 1), because there have been no scoring criteria for the CIRS phantom [13]. The image preference was subjectively assessed and scored as follows: 1 (poor), 2 (not poor), 3 (not good), 4 (good), and 5 (excellent). The scores of specks, mass, and fiber were 12, 7, and 5, respectively.

Two experienced radiologists with 5 and 8 years of experience and also blinded to the information of the phantom images independently evaluated a total of 108 randomly selected images twice. Readers were allowed to adjust the brightness and contrast of the monitor interactively. However, the use of other tools, such as magnification or edge enhancement, was not allowed. A second reading was performed 2 weeks after the completion of the first reading. Any discrepancies between the two readers were resolved by a consensus from the two reading sessions. The final reading score was obtained as a mean value of the scores of the first and second consensus reading.

Statistical analysis

Statistical analyses were performed with SPSS version 13.0 (SPSS Inc., Chicago, USA). The statistical significance of the overall differences between multiple groups was analyzed by one-way ANOVA. The relationships between breast thickness and other variables were calculated by a simple regression analysis. The p values less than 0.05 were considered significant.

RESULTS

Of all features (masses, fibers, and specks) visible in the phantom image, the masses and specks were significantly better visualized in the CNT mode than in other modes ($p < 0.001$ and $p = 0.005$, respectively). However, there was no significant difference between the STN and DOSE modes ($p = 0.168$ and $p = 0.601$, respectively). Moreover, there was no difference in the fiber scores among the three modes. The score of the image preference was highest in the CNT mode ($p < 0.001$) and lowest in the DOSE mode ($p = 0.013$). The scores for all features among the three modes are shown in Table 1 and Figure 2.

All feature scores (masses, fibers, and specks) visible in the phantom image significantly differed among the three glandularity groups (Table 2). However, the score of image preference was not different among the three groups ($p = 0.817$). The scores of masses showed significance in a downward trend with increasing breast glandularity ($p = 0.002$). The score of fibers was highest in the 30% glandular breast tissue groups ($p < 0.001$); however, no difference was found between the 20-21% and 50% glandular breast tissue group ($p = 0.130$). The

http://dx.doi.org/10.4048/jbc.2013.16.1.90

score of specks was lowest in the 50% glandular breast tissue group ($p=0.002$); yet, no difference was found between the 20-21% and 30% glandular breast tissue groups ($p=0.224$). The score of all features was negatively correlated with breast thickness (Table 3), and thus, there was a general downward trend with increasing breast thickness ($p<0.001$). The scores of features among the three modes over a range of breast thickness and glandularity are shown in Figure 3.

The values for AGD, ESE, kVp, and mAs were not significantly different among the three digital mammography systems. We tested the correlation between dose and breast glandularity and found that AGD, ESE, kVp, and mAs were not correlated to breast glandularity (Table 4). However, AGD generally increased with increasing breast thickness. ESE, kVp, and mAs were also positively correlated with breast thickness (Table 5).

Dose measurement among the three modes revealed that AGD was highest in the CNT mode and lowest in the DOSE mode (both, $p<0.001$) (Table 6). Similarly, ESE and mAs values

Table 1. Comparison image quality according to AOP mode

AOP mode	Mass	*p*-value	Fiber	*p*-value	Speck	*p*-value	SIP	*p*-value
STD	4.35±0.52		3.78±0.28		10.78±0.40		4.21±0.45	
CNT	4.92±0.62	<0.001	3.88±0.21	0.096	11.04±0.36	0.005	4.85±0.36	<0.001
DOSE	4.17±0.57	0.168	3.67±0.29	0.076	10.73±0.42	0.601	3.97±0.38	0.013

Data are presented as mean±SD.
AOP=automated optimization of parameters; STD=standard mode; CNT=contrast mode; DOSE=dose mode; SIP=subjective image preference.

Table 2. Comparison of image quality according to the breast glandularity

Glandularity (%)	Mass	Fiber	Speck	SIP
20-21	4.90±0.50	3.61±0.23	11.07±0.19	4.28±0.58
30	4.54±0.46	3.95±0.13	10.93±0.21	4.33±0.54
50	4.30±0.74	3.71±0.30	1072±0.52	4.37±0.54
p-value	0.002	<0.001	0.002	0.817

Data are presented as mean±SD.
SIP=subjective image preference.

Table 3. Correlation of image quality according to the breast thickness

	Coefficient (regression slope)	95% CI		*p*-value
		LB	UB	
Mass	-0.33	-0.47	-0.18	<0.001
Fiber	-0.16	-0.22	-0.11	<0.001
Speck	-0.23	-0.32	-0.14	<0.001
SIP	-0.30	-0.30	-0.42	<0.001

CI=confidence interval; LB=lower bound; UB=upper bound; SIP=subjective image preference.

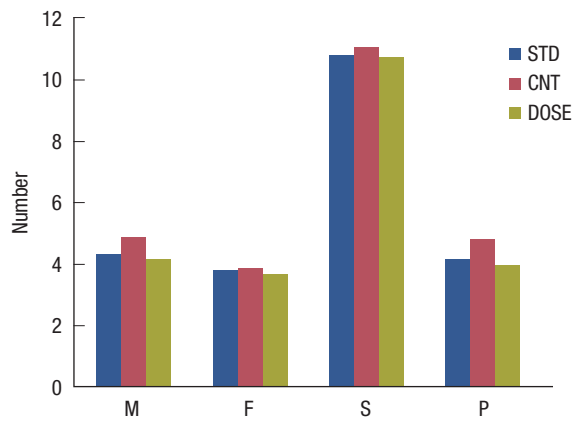

Figure 2. The image quality of all types among the three modes. Image quality is the number of fibers, specks, masses visualized, or image preference.
STD=standard mode; CNT=contrast mode; DOSE=dose mode; M=mass; F=fiber; S=specks; P=image perference.

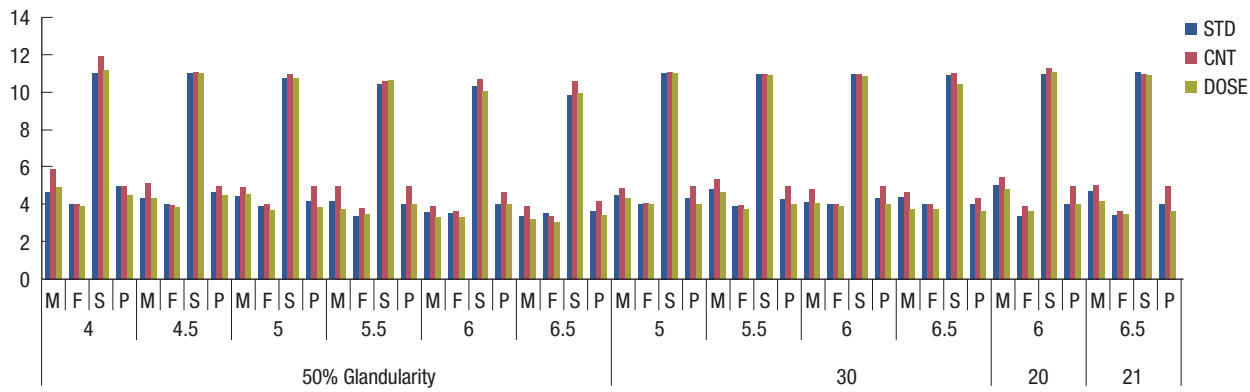

Figure 3. Relationship between image quality and breast thickness.
STD=standard mode; CNT=contrast mode; DOSE=dose mode; M=mass; F=fiber; S=specks; P=image perference.

Table 4. Comparison of AGD, ESE, kVp, and mAs according to the breast glandularity

Glandularity (%)	AGD (mGy)	ESE (mC/kg)	kVp	mAs
20-21	1.57±0.46	7.29±2.15	29.17±0.38	70±23.61
30	1.53±0.48	6.87±2.38	29.08±0.8	67.71±24.65
50	1.45±0.49	6.55±2.24	28.83±1.10	66.37±26.95
p-value	NS	NS	NS	NS

Data are presented as mean±SD.
AGD=average glandular dose; ESE=entrance surface exposure; mAs=milliampere-seconds; NS=not significant.

Table 5. Correlation of AGD, ESE, kVp, and mAs according to the breast thickness

	Coefficient (regression slope)	95% CI		*p*-value
		LB	UB	
AGD	0.13	0.02	0.25	0.023
ESE	1.33	0.81	1.86	<0.001
kVp	0.75	0.61	0.88	<0.001
mAs	7.70	1.74	13.66	0.013

AGD=average glandular dose; ESE=entrance surface exposure; mAs=milliampere-seconds; CI=confidence interval; LB=lower bound; UB=upper bound.

Table 6. Comparison AGD, ESE, kVp, and mAs according to AOP mode

AOP mode	AGD (mGy)	*p*-value	ESE (mC/kg)	*p*-value	kVp	*p*-value	mAs	*p*-value
STD	1.31±0.17		5.98±1.22		28.94±0.79		58.64±9.92	
CNT	2.12±0.18	<0.001	9.62±1.60	<0.001	28.78±0.68	0.381	99.08±14.29	<0.001
DOSE	1.06±0.12	<0.001	4.76±0.90	<0.001	29.19±0.92	0.190	44.64±6.02	<0.001

Data are presented as mean±SD.
AGD=average glandular dose; ESE=entrance surface exposure; mAs=milliampere-seconds; AOP=automated optimization of parameters; STD=standard mode; CNT=contrast mode; DOSE=dose mode.

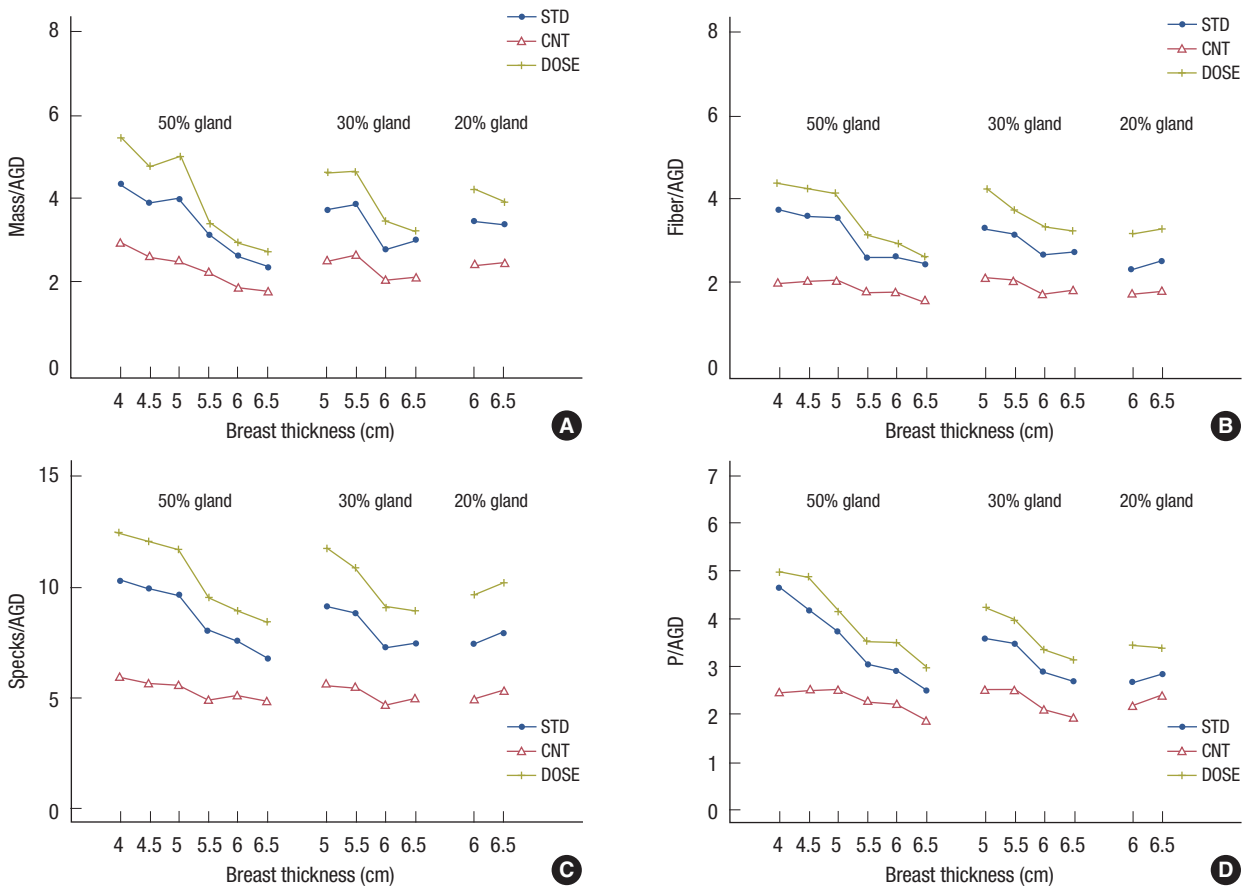

Figure 4. (A-D) The relationship between the image quality over a range of breast thickness and glandularity according to the automatic optimization of parameters (AOP) modes. Image quality is the dose-normalized scores of fibers, specks, masses visualized, or image preferences (lesion scores/average glandular dose [AGD]).
STD=standard mode; CNT=contrast mode; DOSE=dose mode.

http://dx.doi.org/10.4048/jbc.2013.16.1.90

were significantly different among the three modes (both, $p < 0.001$).

ESE was highest in the CNT mode ($p < 0.001$) and lowest in the DOSE mode ($p < 0.001$). The mAs value was also significantly different among STD, CNT and DOSE modes (both, $p < 0.001$). However, the values for kVp did not significantly differ among the three modes (Table 6). The lesion scores were normalized by AGD over the range of breast thickness and glandularity, according to the AOP modes, as shown in Figure 4.

DISCUSSION

The purpose of radiographic technique optimization is to establish standardized imaging protocols by balancing image quality and dose, which is particularly important for screening mammography, given the lifetime risk to women who undergo annual mammography examinations. Without evidence that the image quality improvements at a higher dose would guarantee a clinically significant increase in the diagnostic performance, the more conservative route of favoring dose reduction while maintaining acceptable image quality should be followed [3]. For this reason, the primary objective of our study was to evaluate the dose difference and the difference of image quality among three AOP modes, STD, CNT, and DOSE mode, in order to provide useful information for proper selection of automatic optimized techniques specific to digital mammography.

Although the operator can select one mode of the three AOP modes, the STD mode was routinely used for patient examinations. Hence, CNT and DOSE modes were unfamiliar and their characteristics were not well known. In this study of using three AOP modes, AGD and ESE of the DOSE mode were significantly lowest among the three modes, as expected. AGD and ESE of the DOSE mode is reduced by 19.1% and 25%, respectively, compared to those of the STD mode. However, the image quality did not significantly differ between the DOSE and STD modes, although the image of the STD mode was more preferred to that of the DOSE mode by radiologists. The AGD of the DOSE mode is half of that of CNT and nearly one third of the upper limit of the recommended radiation dose of ACR. As far as image quality is concerned, the score of masses and specks of the DOSE mode was reduced by 15% and 2.8%, respectively, compared to those of the CNT mode. And the score of fibers was not significantly different among three modes. This means that the DOSE mode will be more suitable for screening mammographic examinations considering dose saving and similar image quality to the STD mode. This is of practical importance because the DOSE mode compared to the STD mode has the potential to reduce the risk of cumulative radiation exposure without compromising to the lesion detection rates in patients who undergo annual mammography.

The characterization of masses and microcalcifications are very important and should not compromise to the dose reduction. Hence, for the examination of diagnostic mammography, particularly for the evaluation of mass or microcalcifications, the CNT mode will be more suitable.

Regarding the exposure factors, the mAs level was significantly highest in the CNT mode and lowest in the DOSE mode, similar to AGD and ESE. However, the kVp level was not significantly different among the three modes. This implies that mAs primarily impacts the dose difference among the modes. This result was supported by the previous study [7], which demonstrated that mAs selection among the three AOP modes accounted for the corresponding dose difference amongst them.

Compressed breast thickness and glandularity were important factors affecting AGD [3,7-9]. AGD was calculated using the entrance skin air kerma value and G factor. G factor depends on the breast thickness. Therefore, as compressed breast thickness increased, AGD increased. The average absorbed dose in the glandular breast tissue is the preferred quantity for assessing radiation risk during mammography [14]. In addition, as glandular tissue increases, increased penetration, i.e., high exposure, is necessary [15]. Hence, as glandular tissue increased, the overall absorbed dose increased. In this study, AGD was also significantly correlated with breast thickness. However, AGD was significantly not correlated with glandularity. The target-filter combination for breast thickness ≤ 4.5 cm (i.e., 4 and 4.5 cm) with 50% glandularity was molybdenum-rhodium (Mo-Rh). This combination switched automatically to Rh-Rh for breast thickness > 4.5 cm (i.e., 5, 5.5, 6, and 6.5 cm) regardless of breast glandularity and the selected mode. This change occurred in the same way among the three machines. These findings indicated that the automatic selection of the target/filter combination during image acquisition by the AOP mode is based mainly on breast thickness and is thus relatively insensitive to breast glandularity.

Previous studies [3,8] evaluating the image quality and dose reduction in digital mammography used the physical measures of image quality (i.e., signal difference-to-noise ratio). In contrast, we used the observer performance in our study for evaluating the image quality. Although this is a subjective measurement, the evaluation can provide more practical information as to the difference of image quality in a clinical setting. Our study revealed, against expectations, that the DOSE mode provided an acceptable image quality similar to that of the

STD mode in practice, in addition to the lowest radiation dose; moreover, the DOSE mode can be routinely used in patient examinations.

However, our study had several limits. First, we used the breast phantom for a dosimetry evaluation. The phantoms used for this evaluation had a uniform background with a noise characteristic that is not a representative of the anatomical background encountered in clinical mammography studies. Yet, the phantom study is widely used to compare different imaging systems and image acquisition setups due to its ease and reproducibility [12,16-18]. It seemed therefore reasonable to use standard phantoms to obtain an estimate of a possible dose reduction factor. However it is not as reliable in evaluating the radiation risk as is the patient method, nevertheless employing a phantom with a more anatomically realistic background. Second, we used the digital mammography system made by one manufacture, GE. There are many factors (tube target material, amount and type of filtration, tube's operating voltage, X-ray absorber thickness and material, etc.) involved in determining both the image quality and dose. For that reason the optimum exposure parameters are system specific. Hence, this result is not suitable for all examinations and therefore, further investigation with a different system made by different manufactures will be needed. Third, the scoring was determined by two radiologists in consensus; interobserver variability and intraobserver variability were not evaluated.

Dose reduction balanced with an image quality is particularly important in digital mammography because of the lifetime risk to women who undergo annual mammography examinations. Thus, it is important to know the optimized imaging techniques of digital mammography systems, many of which employ automatic controls. We have presented practical and useful information for the proper selection of exposure mode at clinics. Of the three AOP modes provided by the GE senographe digital system, the DOSE mode offers a significant improvement (19.1-50%) in dose over the other two modes for breast thickness ranging from 4 to 6.5 cm at glandularity ranging from 20% to 50% with an acceptable image quality. The CNT mode provides the highest image quality of masses and specks among the three AOP modes with the highest AGD. Having knowledge of the three AOP modes may reduce unnecessary radiation exposure by utilizing the proper mode according to each purpose.

CONFLICT OF INTEREST

The authors declare that they have no competing interests.

REFERENCES

1. Jemal A, Siegel R, Ward E, Hao Y, Xu J, Thun MJ. Cancer statistics, 2009. CA Cancer J Clin 2009;59:225-49.
2. Vinnicombe S, Pinto Pereira SM, McCormack VA, Shiel S, Perry N, Dos Santos Silva IM. Full-field digital versus screen-film mammography: comparison within the UK breast screening program and systematic review of published data. Radiology 2009;251:347-58.
3. Ranger NT, Lo JY, Samei E. A technique optimization protocol and the potential for dose reduction in digital mammography. Med Phys 2010; 37:962-9.
4. Samei E, Dobbins JT 3rd, Lo JY, Tornai MP. A framework for optimising the radiographic technique in digital X-ray imaging. Radiat Prot Dosimetry 2005;114:220-9.
5. Yaffe MJ, Mainprize JG. Detectors for digital mammography. Technol Cancer Res Treat 2004;3:309-24.
6. Huda W, Sajewicz AM, Ogden KM, Dance DR. Experimental investigation of the dose and image quality characteristics of a digital mammography imaging system. Med Phys 2003;30:442-8.
7. Chen B, Wang Y, Sun X, Guo W, Zhao M, Cui G, et al. Analysis of patient dose in full field digital mammography. Eur J Radiol 2012;81:868-72.
8. Williams MB, Raghunathan P, More MJ, Seibert JA, Kwan A, Lo JY, et al. Optimization of exposure parameters in full field digital mammography. Med Phys 2008;35:2414-23.
9. Bor D, Tukel S, Olgar T, Aydin E. Variations in breast doses for an automatic mammography unit. Diagn Interv Radiol 2008;14:122-6.
10. Berns EA, Hendrick RE, Cutter GR. Performance comparison of full-field digital mammography to screen-film mammography in clinical practice. Med Phys 2002;29:830-4.
11. Ministry of Health and Welfare. Recommendations of Radiation Dose to Patients from Mammography. Seoul: Ministry of Health and Welfare; 2008. p.1-46.
12. Pachoud M, Lepori D, Valley JF, Verdun FR. A new test phantom with different breast tissue compositions for image quality assessment in conventional and digital mammography. Phys Med Biol 2004;49:5267-81.
13. American College of Radiology, Committee on Quality Assurance in Mammography. Mammography Quality Control Manual: Radiologist's Section, Clinical Image Quality, Radiologic Technologist's Section, Medical Physicist's Section. Revised ed. Reston: American College of Radiology; 1999.
14. Statement from the 1987 Como meeting of the International Commission on Radiological Protection. Radiology 1988;167:263-5.
15. Ozdemir A. Clinical evaluation of breast dose and the factors affecting breast dose in screen-film mammography. Diagn Interv Radiol 2007; 13:134-9.
16. Pisano ED, Britt GG, Lin Y, Schell MJ, Burns CB, Brown ME. Factors affecting phantom scores at annual mammography facility inspections by the U.S. Food and Drug Administration. Acad Radiol 2001;8:864-70.
17. Obenauer S, Hermann KP, Grabbe E. Dose reduction in full-field digital mammography: an anthropomorphic breast phantom study. Br J Radiol 2003;76:478-82.
18. Gennaro G, Katz L, Souchay H, Alberelli C, di Maggio C. Are phantoms useful for predicting the potential of dose reduction in full-field digital mammography? Phys Med Biol 2005;50:1851-70.

http://dx.doi.org/10.4048/jbc.2013.16.1.90